Stem Cell Reports
Report

ISSCR

OPEN ACCESS

Direct Lineage Conversion of Adult Mouse Liver Cells and B Lymphocytes to Neural Stem Cells

John P. Cassady,[1,2] Ana C. D'Alessio,[1] Sovan Sarkar,[1] Vardhan S. Dani,[3] Zi Peng Fan,[1,4] Kibibi Ganz,[1] Reinhard Roessler,[1] Mriganka Sur,[3] Richard A. Young,[1,2] and Rudolf Jaenisch[1,2,*]

[1]The Whitehead Institute for Biomedical Research, Cambridge, MA 02142, USA
[2]Department of Biology, Massachusetts Institute of Technology, Cambridge, MA 02139, USA
[3]Department of Brain and Cognitive Sciences, Picower Institute for Learning and Memory, Massachusetts Institute of Technology, Cambridge, MA 02139, USA
[4]Computational and Systems Biology Program, Massachusetts Institute of Technology, Cambridge, MA 02139, USA
*Correspondence: jaenisch@wi.mit.edu
http://dx.doi.org/10.1016/j.stemcr.2014.10.001

SUMMARY

Overexpression of transcription factors has been used to directly reprogram somatic cells into a range of other differentiated cell types, including multipotent neural stem cells (NSCs), that can be used to generate neurons and glia. However, the ability to maintain the NSC state independent of the inducing factors and the identity of the somatic donor cells remain two important unresolved issues in trans-differentiation. Here we used transduction of doxycycline-inducible transcription factors to generate stable tripotent NSCs. The induced NSCs (iNSCs) maintained their characteristics in the absence of exogenous factor expression and were transcriptionally, epigenetically, and functionally similar to primary brain-derived NSCs. Importantly, we also generated tripotent iNSCs from multiple adult cell types, including mature liver and B cells. Our results show that self-maintaining proliferative neural cells can be induced from nonectodermal cells by expressing specific combinations of transcription factors.

INTRODUCTION

Factor-mediated reprogramming, the process by which overexpression of a defined set of transcription factors converts one cell type into another, has important implications for regenerative medicine and demonstrates the power that transcription factors have as cell fate determinants (Jaenisch and Young, 2008). This has been shown for pluripotent stem cells, where three transcription factors (*Oct4*, *Sox2*, and *Klf4*) are sufficient to induce any cell type to become induced pluripotent stem cells (iPSCs) that are transcriptionally, epigenetically, and functionally indistinguishable from embryonic stem cells (ESCs) (Takahashi and Yamanaka, 2006; Wernig et al., 2008a).

Ectopic expression of key transcription factors in somatic donor cells has been used to generate many different cell types, including cells resembling blood cells (Heyworth et al., 2002; Xie et al., 2004), brown fat cells (Kajimura et al., 2009), hepatocytes (Huang et al., 2011), Sertoli cells (Buganim et al., 2012), and various cell types of the neural lineage (Vierbuchen et al., 2010; Kim et al., 2011; Son et al., 2011; Yang et al., 2013). An important advance has been the generation of neural stem cells (NSCs) from embryonic fibroblasts, as these self-renewing somatic stem cells can be expanded for use in clinical application (Lujan et al., 2012; Han et al., 2012; Ring et al., 2012). However, a number of issues remained unresolved and are the focus of this paper. In these studies, the induced NSCs (iNSCs) were still dependent on the constitutive factor expression. Importantly, because the published studies used a heterogeneous population of mouse embryonic fibroblasts (MEFs) as starting cells, it has been difficult to ascertain that indeed nonneural somatic cells gave rise to the iNSCs rather than preexisting neural cells (such as neural crest cells) present in the donor population. Finally, an extensive epigenetic analysis has not been performed on iNSCs, or any other directly converted cell type, to determine whether the chromatin has been reset to allow for cell type-specific gene expression to persist in the absence of the exogenous factors.

Here we show that transient overexpression of 8 transcription factors—*Brn2*, *Hes1*, *Hes3*, *Klf4*, *Myc*, *Notch1*, (*NICD*), *PLAGL1*, and *Rfx4*—in fibroblasts generates iNSCs that can differentiate into neurons, astrocytes, and oligodendrocytes and have similar genome-wide gene expression patterns and enhancer usage as primary-derived control NSC lines. We then used iPSC technology to generate a genetic system that converts multiple adult cell types to tripotent iNSCs, including liver cells and B cells that carry rearrangements in the immunoglobulin loci. Our results indicate that specific combinations of transcription factors can reset the genome of diverse cell types to that of NSCs.

RESULTS

Induction of iNSCs from MEFs

We generated doxycycline (dox)-inducible lentiviruses (Brambrink et al., 2008) that carried factors thought to be

important for NSCs (Bylund et al., 2003; Elkabetz et al., 2008; Imayoshi et al., 2010) and transduced them into fibroblasts carrying a GFP reporter in the *Sox2* locus (*Sox2*-GFP) (Ellis et al., 2004). Initial experiments in which transduced MEFs were cultured in the presence of dox and then monitored for *Sox2*-GFP expression after dox withdrawal were unsuccessful. However, a modified strategy that included dox withdrawal from cells transiently grown in insulin, transferrin, selenium, and fibronectin (ITSFn) medium, which selects for NESTIN-expressing NSCs during in vitro differentiation of ESCs (Okabe et al., 1996), generated multiple lines of *Sox2*-GFP$^+$ cells with a morphology resembling that of control NSCs (Figures S1A and S1B available online). Quantitative PCR (qPCR) analysis confirmed that fibroblast genes were silenced and NSC genes were activated (Figure S1C). Importantly, upon growth factor withdrawal, these cell lines differentiated and stained for neuronal marker TUJ1 and glial marker GFAP (Figure S1D).

To determine the factors responsible for generating self-maintaining iNSC lines, we used PCR to identify the proviral transgenes carried in the genome of iNSC lines. We utilized primers that either spanned introns or, for single-exon genes, amplified between the TetO lentiviral promoter and the gene of interest. We found that between 13 and 21 different proviruses had integrated into the various iNSC lines (Figure S1E).

To identify essential factors, we focused on iNSC5, the line with the fewest number of proviruses. MEFs were transduced with the 13 factors carried in iNSC5—*Sox2*, *Hes1*, *Hes3*, *Brn2*, *Klf4*, *Rfx4*, *Zic1*, *DN-REST*, *NICD*, *Lhx2*, *PLAGL1*, *Myc*, and *Bmi1*—without (13F) or with (14F) *Foxg1*, which was reported to be important for creating dox-dependent iNSCs (Lujan et al., 2012). To determine the minimal duration of factor expression needed to induce transdifferentiation, the cells were cultured in dox for different lengths of time (Figure 1A). iNSCs appeared only after 30 days on dox in both 13F and 14F cultures (Figure 1A) and displayed morphologies and *Sox2*-GFP expression patterns similar to brain-derived control NSCs (Figures 1B and 1C). The cells proliferated in response to epidermal growth factor (EGF)/fibroblast growth factor (FGF) signaling and were able to be expanded for more than 20 passages with similar growth properties as control NSCs (Figure 1D). qPCR revealed that iNSCs expressed NSC genes *Brn2, Sox2* and *Pax6*, but had silenced MEF genes such as *Col5a2* and *Thy1* (Figures 1E).

To functionally characterize the iNSCs, we assessed their capacity to differentiate into neurons, astrocytes, and oligodendrocytes by growing them in previously defined conditions (Thier et al., 2012; Lujan et al., 2012). When EGF/FGF were withdrawn from the growth medium and replaced by BDNF, NT3, and ascorbic acid, the cells differentiated into neurons that stained for TUJ1 and MAP2 (Figure 1F). Whole-cell patch clamp recordings revealed that iNSC-derived neurons differentiated for 4 weeks exhibited action potential firing and voltage-gated ion currents, suggesting excitable membrane properties typical of developing neurons (Figure 1G). The iNSCs also differentiated into GFAP$^+$ astrocytes when the medium was supplemented with 5% serum, and growth in oligodendrocyte-inducing conditions (Glaser et al., 2007) promoted differentiation to O4$^+$ oligodendrocytes (Figure 1F). Control NSCs were differentiated in parallel and showed similar results for each differentiation condition (Figure 1F). Finally, to determine whether iNSCs remained tripotent after numerous passages, passage (P) 20 iNSCs were subjected to the same differentiation conditions, and they retained the ability to differentiate into neurons, astrocytes, and oligoendrocytes (Figure 1F). Thus, the iNSCs possessed the self-renewal and tripotency characteristics associated with NSCs.

iNSCs Are Transcriptionally and Epigenetically Similar to Primary NSCs

Global gene expression and chromatin analysis were performed to characterize the iNSCs on a molecular level. Figure 2A shows that iNSCs had similar global gene expression patterns as ESC-derived neural precursor cells (NPCs) (Mikkelsen et al., 2008) and control NSCs derived from the same genetic background as the iNSCs. This was confirmed by hierarchical clustering and Pearson analysis, which showed that iNSC global gene expression patterns clustered with control NSCs and NPCs and were distinct from fibroblasts and differentiated neural cell types (Figure 2B).

Enhancers are epigenetically marked by histone H3 lysine K27 acetylation (H3K27ac) and display unique cell type-specific profiles (Creyghton et al., 2010). To examine the epigenetic state of iNSCs, H3K27ac chromatin immunoprecipitation (ChIP)-seq was performed on MEFs, control NSCs, and iNSCs. Analysis revealed that iNSCs had a profile similar to control NSCs at many key neural loci such as *Olig1*/*Olig2* (Figure 2C), but dissimilar from MEFs at loci expressed in fibroblasts like *Col3a1/Col5a2* (Figure 2D). Finally, genome-wide analysis showed that iNSCs had a global active enhancer pattern similar to control NSCs and different from the starting population of MEFs (Figure 2E). This was confirmed for a number of loci (Figures S2A and S2B). Thus, iNSCs had transcriptionally and epigenetically reprogrammed their nucleus to a state that was very similar to control NSCs and distinct from the MEF starting population.

A Genetically Homogenous System for Efficient iNSC Induction

To assess the reproducibility of iNSC formation, we developed a "secondary" system (Wernig et al., 2008b) in which dox-inducible vectors were carried in all cells of chimeras

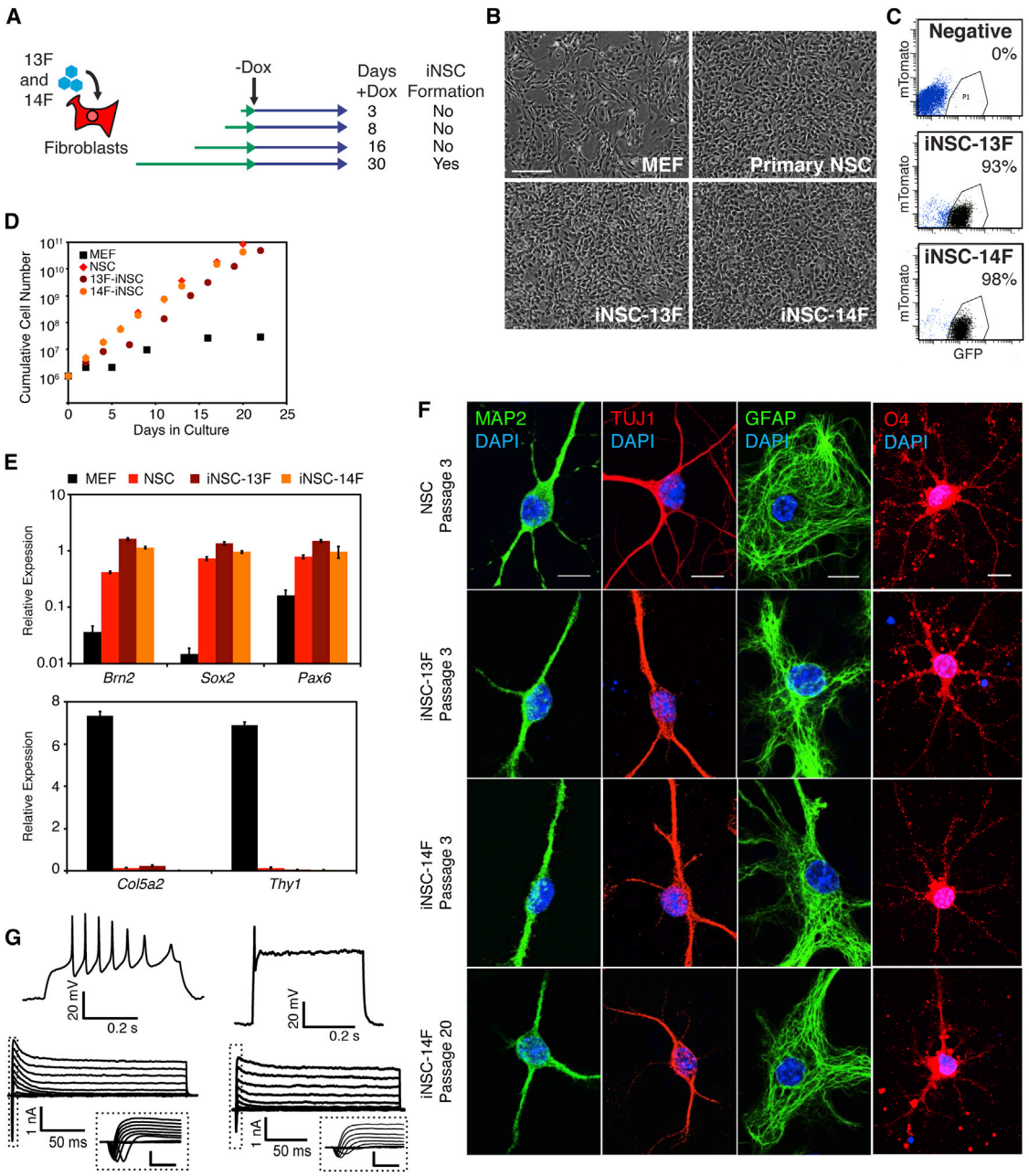

Figure 1. Generation of Transgene-Independent iNSCs

(A) Time course of dox induction. MEFs carrying the *Sox2*-GFP and *Rosa26*-M2rtTA alleles were transduced with the 13 factors (13F) present in iNSC5 (see Figure S1E) or the 13 factors plus *Foxg1* (14F) and grown in the presence of dox for the indicated lengths of time.

(B) Morphology of MEFs (P1), a primary-derived control NSC line, iNSC-13F, and iNSC-14F (each at P3). The scale bar represents 100 μm.

(C) GFP fluorescence of iNSC-13F and iNSC-14F cultures (P3) compared with cells negative for the *Sox2*-GFP reporter (negative). mTomato was used to control for autofluorescence.

(D) Growth curves of MEF, control NSC, iNSC-13F, and iNSC-14F cultures. One million cells were plated on day 0 and cultured continuously for the indicated times.

(E) qPCR analysis of NSC (top) and MEF (bottom) transcript expression in MEFs, control NSCs, iNSC-13F, and iNSC-14F (all P2). Expression values were normalized to *Gapdh* expression for each cell type. Error bars represent SD (n = 3 technical replicates).

(F) Immunostaining for differentiation markers MAP2, TUJ1 (neurons), GFAP (astrocytes), and O4 (oligodendrocytes) after 10–14 days of differentiation. The scale bar represents 10 μm.

(legend continued on next page)

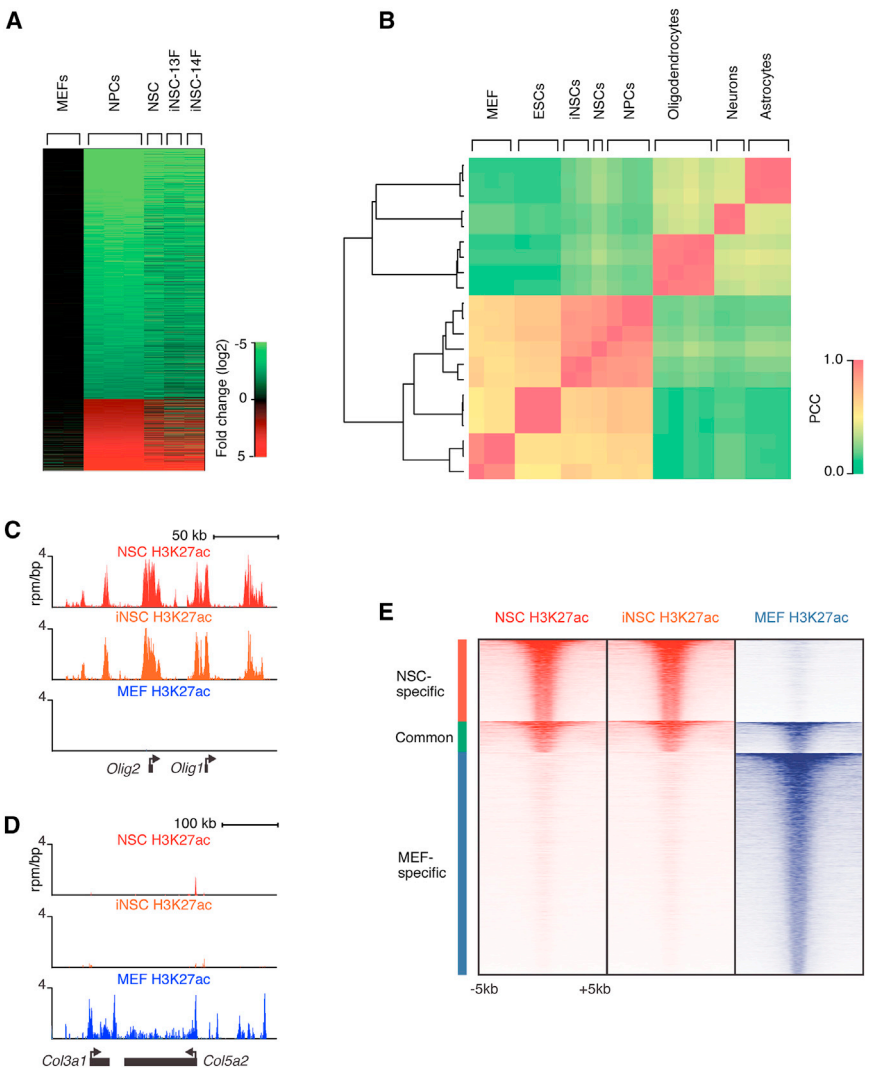

Figure 2. Transcriptional and Epigenetic Reprogramming of iNSCs

(A) Global gene expression analysis comparing the untransduced MEF starting population (P3), primary-derived control NSCs, iNSC-13F, and iNSC-14F (all P8). The heatmap indicates the fold change (log2) of gene expression relative to MEFs. Differentially expressed genes were determined by comparing published ESC-derived NPC and MEF data sets and arranged in rows (Mikkelsen et al., 2008).

(B) Hierarchical clustering and Pearson correlation analysis of gene expression in iNSCs (iNSC-13F and iNSC-14F), control NSCs, ESCs, ESC-derived NPCs, differentiated neural cell lineages, and MEFs (Mikkelsen et al., 2008; Cahoy et al., 2008). The color indicates the Pearson correlation coefficient (PCC).

(C and D) H3K27ac ChIP-seq profiles of the *Olig1/Olig2* locus (C) or the *Col3a1/Col5a2* locus (D) in control NSCs, iNSC-13F (iNSC) (both P8), and MEFs (P3).

(E) Heat map representation of enhancer-associated histone modification H3K27ac at the union of 16,706 enhancer regions from NSCs and MEFs. The enhancer regions were grouped into NSC-specific, common, and MEF-specific enhancers. Read density surrounds the center (±5 kb) of enhancer regions, rank ordered from highest to lowest average H3K27ac occupancy within each group.

See also Figure S2.

and allowed transdifferentiation in the absence of virus transduction (Figure 3A). For this, iNSC-14F cells were reprogrammed to pluripotency using retroviral vectors (Figure S3A). The resulting clonal iPSCs (14F-iPS) carried eight transcription factors—*Brn2*, *Hes1*, *Hes3*, *Klf4*, *Myc*, *NICD*, *PLAGL1*, and *Rfx4* (Figure S3B)—and were pluripotent, generating teratomas and contributing to chimera formation (Figures S3C and S3D). Secondary MEFs were isolated from E14.5 chimeras after removal of neural tissue and selection for puromycin resistance. When cultured in the presence of dox, these cells activated the transgenes and readily transdifferentiated into secondary iNSCs, whereas cells that had never been exposed to dox did not (Figures S3E and S3F). Secondary iNSCs displayed similar morphology, growth properties, and gene expression pattern as the original iNSC line and control NSCs (Figures S3F and S3G) and were also capable of differentiating into neurons and glia (Figure S3H).

Conversion of Adult Liver Cells to iNSCs

Although the secondary system is a robust tool for converting MEFs to iNSCs, control-treated MEF cultures contain up

(G) Whole-cell patch clamp recordings from two different iNSC-14F-derived neurons after 4 weeks of differentiation. Evoked action potential(s) in response to an injected depolarizing current pulse (top) and leak subtracted current responses in voltage clamp during graded voltage steps (bottom) are shown. Insets represent initial current response (dotted line) showing voltage-gated, transient, inward (putative sodium) currents. The inset scale bar represents 1 nA and 5 ms.

See also Figure S1.

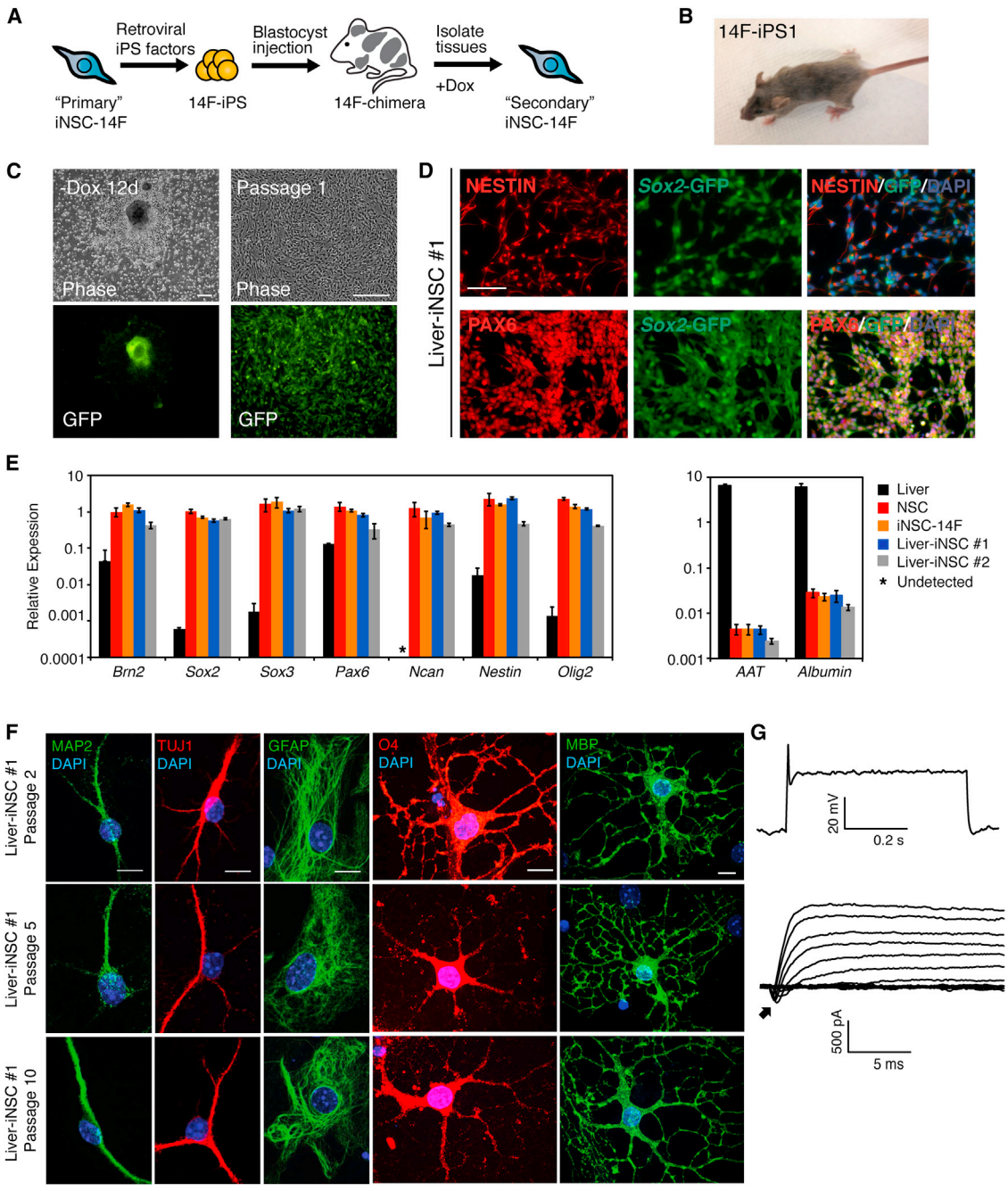

Figure 3. Conversion of Adult Liver Cells to iNSCs

(A) Schematic of strategy to generate an inducible system for generating iNSCs from adult tissues without additional factor transduction.

(B) Adult chimera generated from 14F-iPS1 cell line. The agouti colored hairs arose from the injected iPSCs.

(C) Adult liver cells were explanted from 14F-iPS1 chimera and subjected to iNSC-inducing conditions. Shown are the morphology and *Sox2*-GFP expression of an outgrowth 12 days after dox withdrawal (left) and also after the first passage (right) of Liver-iNSC #1. The scale bar represents 200 μm.

(D) Immunostaining for NESTIN, PAX6, and endogenous *Sox2*-GFP expression in Liver-iNSC #1 (P3). The scale bar represents 100 μm.

(E) qPCR analysis of NSC (left) and liver (right) marker gene expression in whole primary liver, control NSCs, iNSC-14F, and secondary iNSCs derived from adult liver cells (Liver-iNSC #1 and Liver-iNSC #2) (iNSCs at P2). Relative expression is normalized to *Gapdh* for each cell type and the error bars represent SD (n = 3 technical replicates).

(legend continued on next page)

to 1% *Sox2*-GFP$^+$ cells (Lujan et al., 2012; data not shown), which may indicate the presence of neural crest-derived cells in this heterogeneous cell population. Thus, it is possible that the iNSCs were generated from the selection of preexisting neural crest-derived cells rather than by transdifferentiation. To exclude this possibility, we next sought to convert adult liver cells to iNSCs using the secondary system. The liver of an adult 14F-iPS chimera was dissociated and cultured in the presence of dox for iNSC formation (Figures 3B and S3E). The resulting iNSC lines displayed similar morphologies and NESTIN, PAX6, and *Sox2*-GFP expression patterns as control NSCs and other iNSC lines (Figures 3C and 3D). qPCR analysis showed that the liver-derived iNSC lines expressed the NSC markers *Brn2*, *Sox2*, *Sox3*, *Pax6*, *Ncan*, *Nestin*, and *Olig2* to a similar level as control NSCs, but did not express *AAT* or *Albumin*, which are expressed in liver cells (Figure 3E).

Differentiation analysis confirmed that liver-derived iNSCs were tripotent. The cells differentiated into TUJ1$^+$ and MAP2$^+$ neurons that were capable of generating action potentials (Figures 3F and 3G). In the presence of serum, they uniformly differentiated into GFAP$^+$ astrocytes (Figure 3G). In oligodendrocyte-inducing conditions, cells assumed oligodendrocyte-like morphologies and stained for O4 and myelin basic protein (MBP) (Figure 3F). Importantly, the cells remained tripotent at P5 and P10 (Figure 3G). Thus, iNSCs could be generated from adult, non-neural crest-derived cells and had similar molecular features as lines generated from embryonic fibroblasts.

Conversion of B Lymphocytes to iNSCs

Because the liver contains numerous distinct cell types, the molecular identity of the iNSC donor cell remains unknown. To determine whether iNSCs could be induced from a well-defined cell type like B lymphocytes, spleen and bone marrow (BM) cells were isolated from a 14F-iPS chimera and cultured for iNSC formation. Multiple *Sox2*-GFP expressing iNSC lines were generated upon dox induction, whereas none were derived from control-treated cultures (Figure 4A). These iNSC lines had typical NSC morphologies and stained for NESTIN and PAX6 (Figure 4B; data not shown). qPCR analysis confirmed that BM- and spleen-derived iNSCs endogenously expressed the neural transcripts *Brn2*, *Sox2*, *Sox3*, *Nestin*, *Ncan*, and *Olig2*, but not blood cell-associated genes *Pu.1* (*Spi1*) or *Pax5* (Figure 4C). To test the multipotency of these cells, BM- and spleen-derived iNSCs were subjected to differentiation analysis. Similar to previously described iNSCs, these lines could produce TUJ1$^+$ and MAP2$^+$ neurons, GFAP$^+$ astrocytes, and O1$^+$ and O4$^+$ oligodendrocytes (Figures 4D and S4A; data not shown). Finally, whole-cell patch clamp recordings showed that BM-derived iNSCs could differentiate into neurons with excitable membrane properties, such as the expression of voltage-gated ion channels and the ability to generate an action potential (Figure 4E) (note that spleen-derived iNSC neurons were not assessed for membrane properties).

The identity of donor B lymphocytes can be retrospectively ascertained by the DNA rearrangements that occur during maturation (Jung et al., 2006). To determine whether any of the BM- or spleen-derived iNSC lines were induced from a B cell, we isolated genomic DNA and performed PCR analysis for rearrangements of the heavy and light chain immunoglobulin loci (Hanna et al., 2008) (Figure S4B). Analysis of BM-derived line BM-iNSC #1 revealed one D_H-J_H rearrangement that was confirmed by sequencing (Figures 4F and 4G), which is consistent with this line being derived from a Pro-B cell (Hardy and Hayakawa, 2001). Spleen-iNSC #3 had two heavy-chain rearrangements—one productive in-frame V_H-DJ_H and a second D_H-J_H rearrangement—in addition to a productive *Igκ* light-chain locus rearrangement (Figure 4F). The PCR bands were excised, and sequencing confirmed that a donor cell for this iNSC line was a mature B lymphocyte (Figures 4H and S4C) (Hardy and Hayakawa, 2001). Thus, these results confirm that multipotent iNSCs were derived from immature and mature B cells by transdifferentiation.

DISCUSSION

The results described here, using the efficient secondary system to induce transdifferentiation, show that multipotent self-renewing NSCs can be directly derived from a variety of adult somatic donor cells. Our data extend previous reports in three important aspects: (1) Previous studies used heterogeneous MEFs as the donor cell population, which may have contained neural-derived cells. Thus, these data did not exclude the possibility that the iNSCs were derived by outgrowth of these neural cells stimulated by the culture conditions and transduced factors. Here we unambiguously demonstrate, based on immunoglobulin loci

(F) Immunostaining for Liver-iNSC #1-derived neurons (MAP2, TUJ1), astrocytes (GFAP), and oligodendrocytes (O4 and MBP) after 10–14 days of differentiation. Differentiation was assayed at passages 2, 5, and 10. The scale bar represents 10 μm.
(G) Whole-cell recording from a Liver-iNSC #1-derived neuron patched in a culture differentiated for 4 weeks and that showed evoked action potentials in response to injected current (top) and low-amplitude voltage-gated currents (bottom). Arrow points to low amplitude, voltage-gated, transient inward currents.
See also Figure S3.

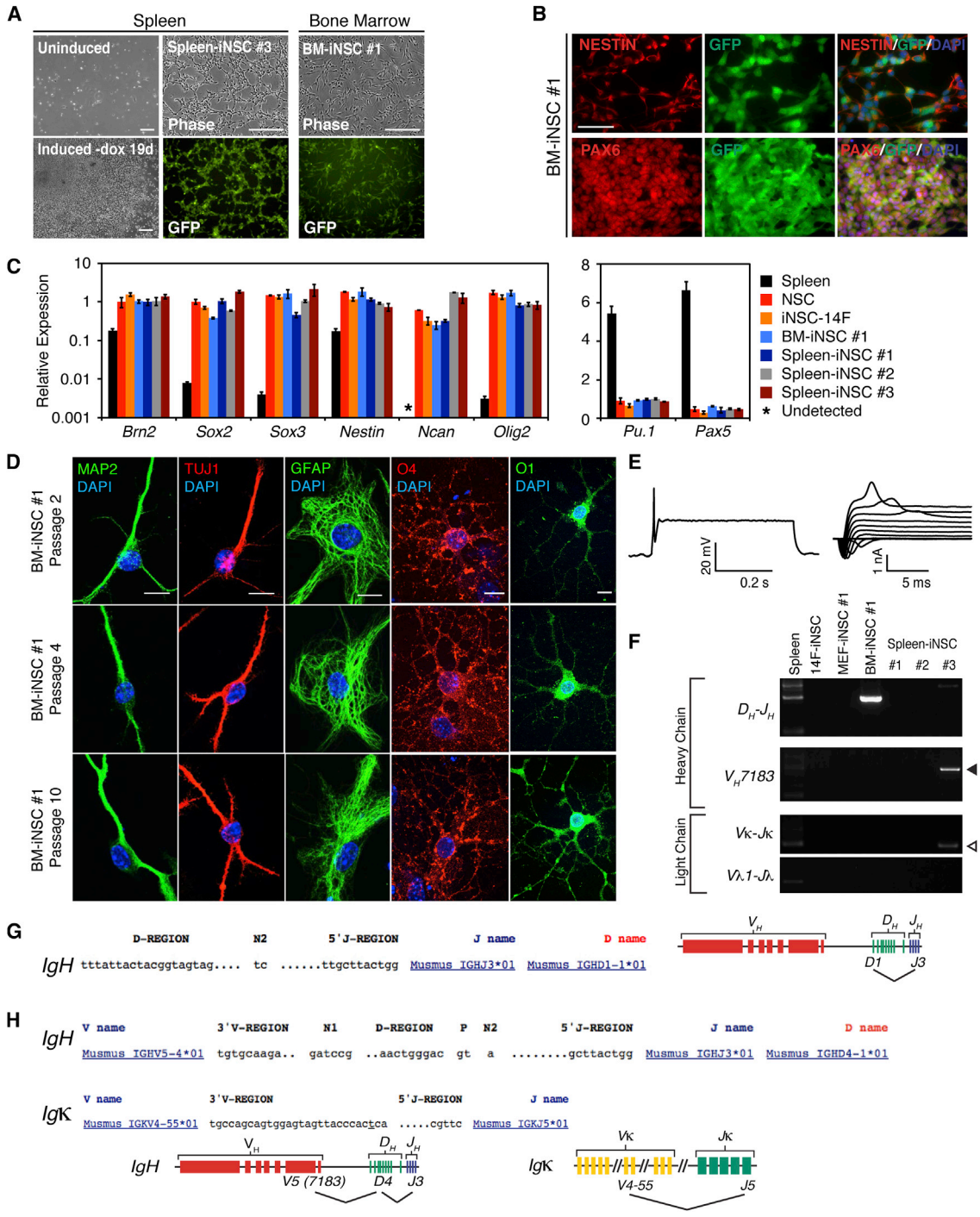

Figure 4. Conversion of Blood Cells to iNSCs

(A) Spleen and BM cells were isolated from 14F-iPS1 adult chimeras. (Left) Comparison of mock-treated spleen cultures (uninduced) and cultures subjected to NSC formation (19 days after dox withdrawal) (Spleen-iNSC #1 is shown). Morphology and GFP fluorescence of Spleen-iNSC #3 and BM-iNSC #1 are shown in the middle and right, respectively. The scale bar represents 200 μm.

(B) Immunostaining for NESTIN, PAX6, and endogenous *Sox2*-GFP expression in BM-iNSC #1 (P3). The scale bar represents 50 μm.

(C) qPCR analysis of NSC (left) and blood (right) marker gene expression in primary spleen, control NSCs, iNSC-14F, and secondary iNSCs derived from BM (BM-iNSC #1) and spleen (Spleen-iNSC #1-3) (iNSCs at P2). Relative expression is normalized to *Gapdh* for each cell type, and the error bars represent SD (n = 3 technical replicates).

(legend continued on next page)

rearrangement as a retrospective genetic marker, that iNSCs can be directly derived from B lymphocytes and from adult liver cells. (2) The maintenance of the iNSC state in previous reports was dependent on the continuous expression of the inducing transcription factors. In contrast, the iNSCs described here are independent of transgene expression. (3) An extensive chromatin and gene expression analysis showed that globally the gene expression and epigenetic states are highly similar to that of control NSCs, and thus, the endogenous NSC regulatory network has been stabilized.

Adult somatic cells have been directly reprogrammed to mature neurons (Vierbuchen et al., 2010; Marro et al., 2011; Son et al., 2011). However, since these cells are post-mitotic, it is difficult to obtain large numbers of cells required for transplantation therapy. The direct conversion of readily accessible adult somatic cells to NSCs is of clinical significance since NSCs can proliferate and thus allow the generation of large quantities of neurons and glia that could be used for eventual transplantation therapy.

EXPERIMENTAL PROCEDURES

iNSC Reprogramming

For the generation of iNSCs, transduced MEFs were grown for 4 days in MEF medium supplemented with 2 μg/ml dox (Sigma), then in neural induction medium (N2 medium [Okabe et al., 1996] plus 10 ng/ml EGF [R&D Systems], 10 ng/ml bFGF [Sigma], 1 μg/ml laminin [Life Technologies], and 2 μg/ml dox) for 2 to 3 weeks before the addition of ITSFn selection medium (Dulbecco's modified Eagle's medium/F-12 medium containing insulin [25 μg/ml], transferrin [50 μg/ml], sodium selenite [30 nM], fibronectin [5 μg/ml; Sigma], and penicillin/streptomycin [100 μg/ml; Life Technologies]) (Okabe et al., 1996), which included dox for the first 4 days. After 10 days in ITSFn (6 days after dox withdrawal), the cells were dissociated and replated onto plates coated with polyornithine (15 μg/ml; Sigma) and laminin (1 μg/ml) and subsequently cultured in neural expansion medium (N2 supplemented with 20 ng/ml EGF, 20 ng/ml bFGF, and 1 μg/ml laminin). *Sox2*-GFP$^+$ cells were sorted directly into polyornithine and laminin-coated plates and split at confluence for P1. All animal procedures were performed according to NIH guidelines and were approved by the Committee on Animal Care at MIT.

ACCESSION NUMBERS

The Gene Expression Ominbus (GEO) accession number for the gene expression and ChIP-seq analyses in this paper is GSE61434.

SUPPLEMENTAL INFORMATION

Supplemental Information includes Supplemental Experimental Procedures and four figures and can be found with this article online at http://dx.doi.org/10.1016/j.stemcr.2014.10.001.

AUTHOR CONTRIBUTIONS

J.P.C. and R.J. conceived this study and wrote the paper. J.P.C., A.C.D., Z.F.P. and R.A.Y. designed, performed, and analyzed ChIP and microarray experiments. S.S. performed confocal microscopy. J.P.C., V.S.D., and M.S. designed and performed electrophysiology experiments. R.R. assisted with electrophysiology differentiations. K.G. performed microinjections. J.P.C. designed and performed all other experiments.

ACKNOWLEDGMENTS

We thank Y. Li, M. Dawlaty, Q. Gao, and J. Hanna for advice; D. Fu and T. Lungjangwa for experimental assistance; and the Whitehead flow cytometry core facility. We are deeply indebted to C. Chen, J. Bland, and J. Huang for their help and encouragement. J.P.C. was supported by a Howard Hughes Medical Institute Gilliam Fellowship. This work was supported by NIH grants HD 045022 and R37CA084198 to R.J., HG002668 to R.Y., and a grant from the Simons Foundation (SFARI 204106 to R.J.). R.J. is a cofounder of Fate Therapeutics and an advisor to Stemgent.

Received: April 6, 2014
Revised: October 1, 2014
Accepted: October 1, 2014
Published: November 6, 2014

REFERENCES

Brambrink, T., Foreman, R., Welstead, G.G., Lengner, C.J., Wernig, M., Suh, H., and Jaenisch, R. (2008). Sequential expression of pluripotency markers during direct reprogramming of mouse somatic cells. Cell Stem Cell *2*, 151–159.

Buganim, Y., Itskovich, E., Hu, Y.-C., Cheng, A.W., Ganz, K., Sarkar, S., Fu, D., Welstead, G.G., Page, D.C., and Jaenisch, R. (2012).

(D) Immunostaining of BM-iNSC #1 cultures at indicated passage differentiated to neurons (MAP2 AND TUJ1), astrocytes (GFAP), or oligodendrocytes (O4 and O1). The scale bar represents 10 μm.
(E) Whole-cell recordings from a BM-iNSC #1-derived neuron patched in a culture differentiated for 4 weeks and that showed evoked action potentials in response to injected current (left) and voltage-gated currents (right).
(F) PCR analysis for heavy-chain (D_H-J_H, V_H*J558*-DJ_H, and V_H*7183*-DJ_H) and light-chain ($V\kappa$-$J\kappa$ and $V\lambda1$-$J\lambda$) recombination event**s** in the genomic DNA of the indicated iNSC lines.
(G) Sequencing analysis of BM-iNSC #1 D_H-J_H rearrangement. The *D* and *J* segments involved in the *IgH* rearrangement are shown (left), as well as a genomic representation of the locus (right).
(H) Sequencing analysis of productive Spleen-iNSC #3 V_H*7183*-DJ_H rearrangement (black arrowhead in part F) (top) and $V\kappa$-$J\kappa$ rearrangement (white arrowhead in part F) (middle). A genomic representation of the *IgH* and *Ig*κ rearrangements is shown.
See also Figure S4.

Direct reprogramming of fibroblasts into embryonic Sertoli-like cells by defined factors. Cell Stem Cell *11*, 373–386.

Bylund, M., Andersson, E., Novitch, B.G., and Muhr, J. (2003). Vertebrate neurogenesis is counteracted by Sox1-3 activity. Nat. Neurosci. *6*, 1162–1168.

Cahoy, J.D., Emery, B., Kaushal, A., Foo, L.C., Zamanian, J.L., Christopherson, K.S., Xing, Y., Lubischer, J.L., Krieg, P.A., Krupenko, S.A., et al. (2008). A transcriptome database for astrocytes, neurons, and oligodendrocytes: a new resource for understanding brain development and function. J. Neurosci. *28*, 264–278.

Creyghton, M.P., Cheng, A.W., Welstead, G.G., Kooistra, T., Carey, B.W., Steine, E.J., Hanna, J., Lodato, M.A., Frampton, G.M., Sharp, P.A., et al. (2010). Histone H3K27ac separates active from poised enhancers and predicts developmental state. Proc. Natl. Acad. Sci. USA *107*, 21931–21936.

Elkabetz, Y., Panagiotakos, G., Al Shamy, G., Socci, N.D., Tabar, V., and Studer, L. (2008). Human ES cell-derived neural rosettes reveal a functionally distinct early neural stem cell stage. Genes Dev. *22*, 152–165.

Ellis, P., Fagan, B.M., Magness, S.T., Hutton, S., Taranova, O., Hayashi, S., McMahon, A., Rao, M., and Pevny, L. (2004). SOX2, a persistent marker for multipotential neural stem cells derived from embryonic stem cells, the embryo or the adult. Dev. Neurosci. *26*, 148–165.

Glaser, T., Pollard, S.M., Smith, A., and Brüstle, O. (2007). Tripotential differentiation of adherently expandable neural stem (NS) cells. PLoS ONE *2*, e298.

Han, D.W., Tapia, N., Hermann, A., Hemmer, K., Höing, S., Araúzo-Bravo, M.J., Zaehres, H., Wu, G., Frank, S., Moritz, S., et al. (2012). Direct reprogramming of fibroblasts into neural stem cells by defined factors. Cell Stem Cell *10*, 465–472.

Hanna, J., Markoulaki, S., Schorderet, P., Carey, B.W., Beard, C., Wernig, M., Creyghton, M.P., Steine, E.J., Cassady, J.P., Foreman, R., et al. (2008). Direct reprogramming of terminally differentiated mature B lymphocytes to pluripotency. Cell *133*, 250–264.

Hardy, R.R., and Hayakawa, K. (2001). B cell development pathways. Annu. Rev. Immunol. *19*, 595–621.

Heyworth, C., Pearson, S., May, G., and Enver, T. (2002). Transcription factor-mediated lineage switching reveals plasticity in primary committed progenitor cells. EMBO J. *21*, 3770–3781.

Huang, P., He, Z., Ji, S., Sun, H., Xiang, D., Liu, C., Hu, Y., Wang, X., and Hui, L. (2011). Induction of functional hepatocyte-like cells from mouse fibroblasts by defined factors. Nature *475*, 386–389.

Imayoshi, I., Sakamoto, M., Yamaguchi, M., Mori, K., and Kageyama, R. (2010). Essential roles of Notch signaling in maintenance of neural stem cells in developing and adult brains. J. Neurosci. *30*, 3489–3498.

Jaenisch, R., and Young, R. (2008). Stem cells, the molecular circuitry of pluripotency and nuclear reprogramming. Cell *132*, 567–582.

Jung, D., Giallourakis, C., Mostoslavsky, R., and Alt, F.W. (2006). Mechanism and control of V(D)J recombination at the immunoglobulin heavy chain locus. Annu. Rev. Immunol. *24*, 541–570.

Kajimura, S., Seale, P., Kubota, K., Lunsford, E., Frangioni, J.V., Gygi, S.P., and Spiegelman, B.M. (2009). Initiation of myoblast to brown fat switch by a PRDM16-C/EBP-beta transcriptional complex. Nature *460*, 1154–1158.

Kim, J., Su, S.C., Wang, H., Cheng, A.W., Cassady, J.P., Lodato, M.A., Lengner, C.J., Chung, C.-Y., Dawlaty, M.M., Tsai, L.H., and Jaenisch, R. (2011). Functional integration of dopaminergic neurons directly converted from mouse fibroblasts. Cell Stem Cell *9*, 413–419.

Lujan, E., Chanda, S., Ahlenius, H., Südhof, T.C., and Wernig, M. (2012). Direct conversion of mouse fibroblasts to self-renewing, tripotent neural precursor cells. Proc. Natl. Acad. Sci. USA *109*, 2527–2532.

Marro, S., Pang, Z.P., Yang, N., Tsai, M.-C., Qu, K., Chang, H.Y., Südhof, T.C., and Wernig, M. (2011). Direct lineage conversion of terminally differentiated hepatocytes to functional neurons. Cell Stem Cell *9*, 374–382.

Mikkelsen, T.S., Hanna, J., Zhang, X., Ku, M., Wernig, M., Schorderet, P., Bernstein, B.E., Jaenisch, R., Lander, E.S., and Meissner, A. (2008). Dissecting direct reprogramming through integrative genomic analysis. Nature *454*, 49–55.

Okabe, S., Forsberg-Nilsson, K., Spiro, A.C., Segal, M., and McKay, R.D. (1996). Development of neuronal precursor cells and functional postmitotic neurons from embryonic stem cells in vitro. Mech. Dev. *59*, 89–102.

Ring, K.L., Tong, L.M., Balestra, M.E., Javier, R., Andrews-Zwilling, Y., Li, G., Walker, D., Zhang, W.R., Kreitzer, A.C., and Huang, Y. (2012). Direct reprogramming of mouse and human fibroblasts into multipotent neural stem cells with a single factor. Cell Stem Cell *11*, 100–109.

Son, E.Y., Ichida, J.K., Wainger, B.J., Toma, J.S., Rafuse, V.F., Woolf, C.J., and Eggan, K. (2011). Conversion of mouse and human fibroblasts into functional spinal motor neurons. Cell Stem Cell *9*, 205–218.

Takahashi, K., and Yamanaka, S. (2006). Induction of pluripotent stem cells from mouse embryonic and adult fibroblast cultures by defined factors. Cell *126*, 663–676.

Thier, M., Wörsdörfer, P., Lakes, Y.B., Gorris, R., Herms, S., Opitz, T., Seiferling, D., Quandel, T., Hoffmann, P., Nöthen, M.M., et al. (2012). Direct conversion of fibroblasts into stably expandable neural stem cells. Cell Stem Cell *10*, 473–479.

Vierbuchen, T., Ostermeier, A., Pang, Z.P., Kokubu, Y., Südhof, T.C., and Wernig, M. (2010). Direct conversion of fibroblasts to functional neurons by defined factors. Nature *463*, 1035–1041.

Wernig, M., Meissner, A., Cassady, J.P., and Jaenisch, R. (2008a). c-Myc is dispensable for direct reprogramming of mouse fibroblasts. Cell Stem Cell *2*, 10–12.

Wernig, M., Lengner, C.J., Hanna, J., Lodato, M.A., Steine, E., Foreman, R., Staerk, J., Markoulaki, S., and Jaenisch, R. (2008b). A drug-inducible transgenic system for direct reprogramming of multiple somatic cell types. Nat. Biotechnol. *26*, 916–924.

Xie, H., Ye, M., Feng, R., and Graf, T. (2004). Stepwise reprogramming of B cells into macrophages. Cell *117*, 663–676.

Yang, N., Zuchero, J.B., Ahlenius, H., Marro, S., Ng, Y.H., Vierbuchen, T., Hawkins, J.S., Geissler, R., Barres, B.A., and Wernig, M. (2013). Generation of oligodendroglial cells by direct lineage conversion. Nat. Biotechnol. *31*, 434–439.

Stem Cell Reports, Volume *3*

Supplemental Information

Direct Lineage Conversion of Adult Mouse Liver Cells and B Lymphocytes to Neural Stem Cells

John P. Cassady, Ana C. D'Alessio, Sovan Sarkar, Vardhan S. Dani, Zi Peng Fan, Kibibi Ganz, Reinhard Roessler, Mriganka Sur, Richard A. Young, and Rudolf Jaenisch

Figure S1

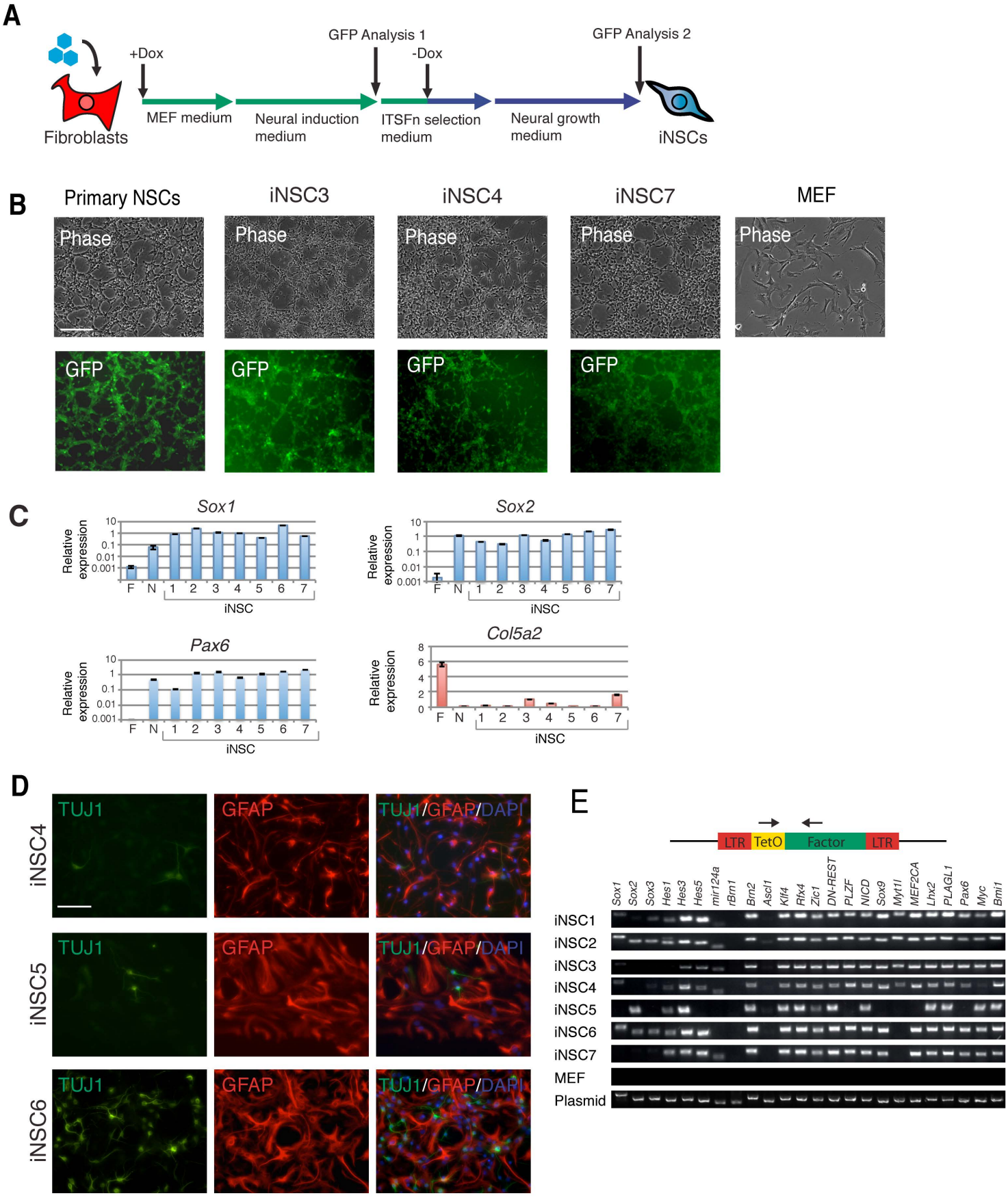
A
+Dox
GFP Analysis 1
-Dox
GFP Analysis 2
Fibroblasts
MEF medium
Neural induction medium
ITSFn selection medium
Neural growth medium
iNSCs
B
Primary NSCs
iNSC3
iNSC4
iNSC7
MEF
Phase
GFP
C
Sox1
Sox2
Pax6
Col5a2
Relative expression
iNSC
F N 1 2 3 4 5 6 7
D
iNSC4
iNSC5
iNSC6
TUJ1
GFAP
TUJ1/GFAP/DAPI
E
LTR
TetO
Factor
LTR
Sox1 Sox2 Sox3 Hes1 Hes3 Hes5 mir124a rBm1 Brn2 Ascl1 Klf4 Rfx4 Zic1 DN-REST PLZF NICD Sox9 Myt1l MEF2CA Lhx2 PLAGL1 Pax6 Myc Bmi1
iNSC1
iNSC2
iNSC3
iNSC4
iNSC5
iNSC6
iNSC7
MEF
Plasmid

Figure S1. Defined growth conditions and factors induce transgene-independent iNSCs

(Related to Figure 1)

(A) Experimental strategy for inducing and selecting transgene-independent NSC-like cells from MEFs. Dox was withdrawn on day 4 of a 10 day growth period in a neural selection medium (ITSFn). See methods section for experimental details.

(B) Morphology and GFP fluorescence of iNSCs generated from transduced MEFs using the experimental strategy shown in part (A). Scale bar=200μm.

(C) qPCR analysis of indicated NSC and MEF transcripts in MEFs (F), primary-derived control NSCs (N), and iNSC lines induced from MEFs. Expression values were normalized to *Gapdh* expression for each cell type, and error bars represent standard deviation from the mean (n=3 technical replicates).

(D) Immunostaining of differentiation markers GFAP and TUJ1 after growth factor withdrawal in representative lines. Scale bar=100μm.

(E) Top, schematic showing the PCR strategy to detect factors transduced in the genomic DNA of iNSC lines. Primer sets either included a universal primer recognizing the TetO promoter and a factor-specific reverse primer, or two factor-specific primers separated by at least one intron in the endogenous gene. Bottom, PCR genotyping results for the transduced factors detected in iNSC lines. The asterisk denotes line iNSC5, which contained the fewest number of transduced factors.

Figure S2

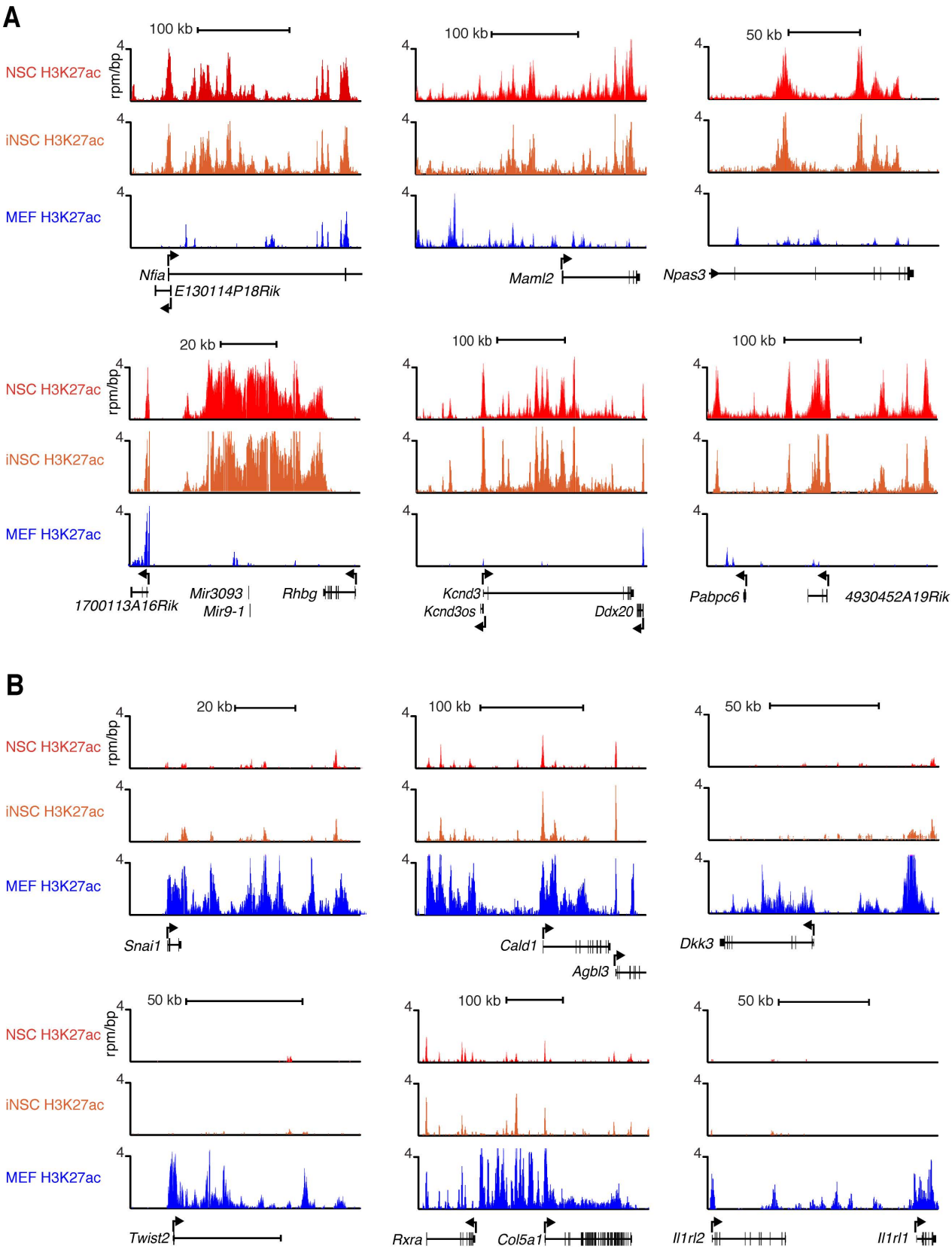
A
100 kb
NSC H3K27ac
iNSC H3K27ac
MEF H3K27ac
rpm/bp
4
Nfia
E130114P18Rik
100 kb
Maml2
50 kb
Npas3
20 kb
1700113A16Rik
Mir3093
Mir9-1
Rhbg
100 kb
Kcnd3
Kcnd3os
Ddx20
100 kb
Pabpc6
4930452A19Rik
B
20 kb
Snai1
100 kb
Cald1
Agbl3
50 kb
Dkk3
50 kb
Twist2
100 kb
Rxra
Col5a1
50 kb
Il1rl2
Il1rl1

Figure S2. H3K27ac profiles at NSC-specific and MEF-specific loci (Related to Figure 2)

(A) H3K27ac ChIP-seq profiles of representative loci with NSC-specific enhancers depicted in Figure 2E. Shown are the profiles for neural-associated transcription factors *Nfia*, *Mastermind-like 2* (*Maml2*), and *Npas3* (top), as well as brain-specific microRNA *miR-9-1*, potassium voltage-gated channel protein gene *Kcnd3*, and the mRNA binding protein *Pacbp6*.

(B) H3K27ac ChIP-seq profiles of representative loci with MEF-specific enhancers depicted in Figure 2E. Shown are profiles for transcription factors *Snai1* and *Twist2* (left), MEF-specific *Caldesmon 1* (*Cald1*) and *Collagen 5a1* (middle), as well as the signaling molecule *Dkk3* and the cytokine receptor gene cluster *Il1lr1/Il1lr2* (right).

Figure S3

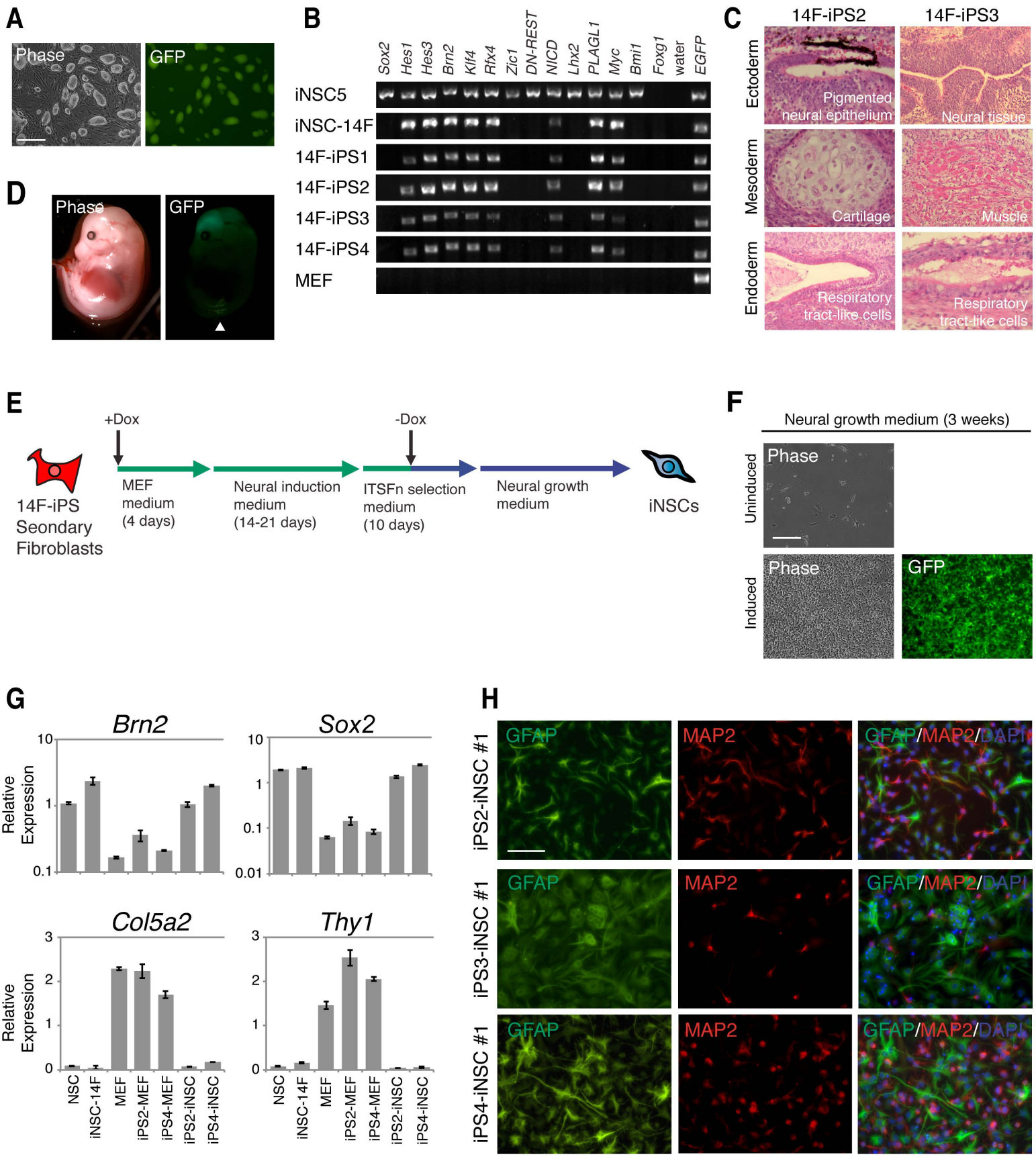
A
Phase
GFP
B
Sox2
Hes1
Hes3
Brn2
Klf4
Rfx4
Zic1
DN-REST
NICD
Lhx2
PLAGL1
Myc
Bmi1
Foxg1
water
EGFP
iNSC5
iNSC-14F
14F-iPS1
14F-iPS2
14F-iPS3
14F-iPS4
MEF
C
14F-iPS2
14F-iPS3
Ectoderm
Mesoderm
Endoderm
Pigmented neural epithelium
Neural tissue
Cartilage
Muscle
Respiratory tract-like cells
Respiratory tract-like cells
D
Phase
GFP
E
+Dox
-Dox
14F-iPS Seondary Fibroblasts
MEF medium (4 days)
Neural induction medium (14-21 days)
ITSFn selection medium (10 days)
Neural growth medium
iNSCs
F
Neural growth medium (3 weeks)
Uninduced
Induced
Phase
Phase
GFP
G
Brn2
Sox2
Col5a2
Thy1
Relative Expression
NSC
iNSC-14F
MEF
iPS2-MEF
iPS4-MEF
iPS2-iNSC
iPS4-iNSC
H
iPS2-iNSC #1
iPS3-iNSC #1
iPS4-iNSC #1
GFAP
MAP2
GFAP/MAP2/DAPI

Figure S3. Genetically homogenous system for iNSC formation

(Related to Figure 3)

(A) ES-like morphology and *Sox2*-GFP expression of iNSC-14F-derived iPS lines. Shown is cell line 14F-iPS1. Scale bar=200μm.

(B) PCR analysis to detect factors integrated in genomic DNA of iNSC-14F and 14F-derived clonal iPS lines (1-4). iNSC5 and untransduced MEFs are shown for reference.

(C) Hematoxylin and eosin staining of teratomas derived from iPS cell lines 14F-iPS2 and 14F-iPS3.

(D) E14.5 chimera derived from blastocyst injection of 14F-iPS4. The GFP fluorescence in the brain and spinal cord (arrowhead) comes from the *Sox2*-GFP reporter of 14F-iPS4 cells.

(E) Schematic for generating secondary iNSCs from 14F-iPS-derived chimera embryonic fibroblasts (Secondary Fibroblasts).

(F) Morphology and *Sox2*-GFP expression at the conclusion of the iNSC induction time course depicted in (E) for both mock-treated cells (Uninduced) and those given dox (Induced). Cells shown in the uninduced condition were non-proliferative and did not express GFP. The cultures were grown in parallel and imaged at the same time. Scale bar=200μm.

(G) qPCR analysis of NSC (*Brn2* and *Sox2*) and fibroblast (*Col5a2* and *Thy1*) marker genes in established secondary iNSC lines (iPS2-iNSC #1 and iPS4-iNSC #1), as well as their starting MEF cultures (iPS2-MEF and iPS4-MEF), a primary-derived control NSC line (NSC), iNSC-14F, and control MEFs. Expression values were normalized to *Actin* expression for each cell type, and error bars represent standard deviation from the mean (n=3 technical replicates).

(H) Immunostaining for GFAP and MAP2 expression in differentiation cultures of 3 independent secondary iNSC lines (iPS2-iNSC #1, iPS3-iNSC #1 and iPS4-iNSC #1). Each secondary iNSC line was derived from MEFs generated after chimera formation using different 14F-iPS clones (iPS2-4). The cultures were analyzed 4 days after growth factor withdrawal. Scale bar=100μm.

Figure S4

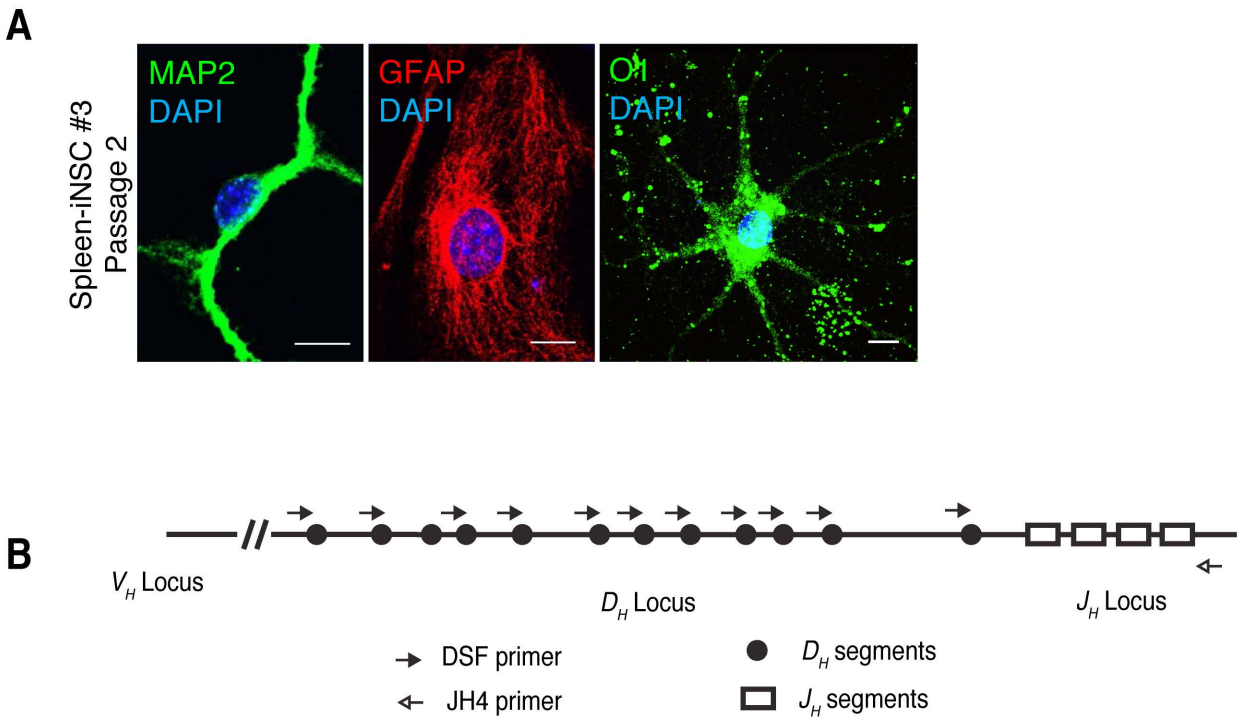
A
Spleen-iNSC #3
Passage 2
MAP2
DAPI
GFAP
DAPI
O4
DAPI
B
V_H Locus
D_H Locus
J_H Locus
DSF primer
JH4 primer
D_H segments
J_H segments
C
D-REGION
P
5'J-REGION
J name
D name
tctatgatggttactac
g
.....ttgactactgg
Musmus IGHJ2*01
Musmus IGHD2-3*01
D2-3
J2

Figure S4. Additional characterization of spleen-derived iNSCs

(Related to Figure 4)

(A) Differentiation analysis of Spleen-iNSC #3 after 10 days of differentiation. Shown are immunostaining for neurons (MAP2), astrocytes (GFAP), and oligodendrocytes (O1). Scale bar=10μm.

(B) PCR strategy for detecting D_H-J_H rearrangements. D_H-J_H rearrangements were amplified using a degenerate PCR primer (DSF) that binds to all D_H-segments and another primer that binds 3' of the J_H4 segment (JH4). The primers only generate a PCR product after genomic rearrangement.

(C) Sequencing analysis of Spleen-iNSC #3 D_H-J_H rearrangement shown in Figure 4F (top panel). The *D* and *J* segments involved in the *IgH* rearrangement are shown (top), as well as a genomic representation of the locus (bottom). Locus not drawn to scale.

SUPPLEMENTAL EXPERIMENTAL PROCEDURES

Somatic cell isolation and culture

Mouse embryonic fibroblasts (MEFs) were isolated from E14.5 embryos that contained two alleles of the M2 reverse tetracycline trans-activator (M2rtTA) in the constitutively active *Rosa26* locus (*Rosa26*-rtTA +/+) (Beard et al., 2006). The embryos also harbored one allele of *Sox2*-GFP in which the endogenous *Sox2* gene was replaced by a sequence encoding eGFP (Ellis et al., 2004). After removing the head, vertebral column, and internal organs, MEFs were dissociated in 0.25% trypsin (Sigma) for 10 minutes, split onto two 15-cm plates, and grown in MEF medium [DMEM supplemented with 10% FBS (Hyclone), penicillin and streptomycin (100 μg/ml) (Life Technologies), L-glutamine (2 mM) (Life Technologies), and nonessential amino acids (Life Technologies)] until confluent and then frozen. MEFs passaged one to two times were used for transduction experiments. MEFs in the secondary iNSC reprogramming experiments were isolated from E14.5 chimeras using the same protocol as above except that chimera cells were selected in medium containing puromycin (2 μg/ml) for 4-6 days.

Adult somatic organs were isolated from 6-week-old chimeric mice as previously described (Carey et al., 2011; Carey et al., 2010). Whole bone marrow was isolated by removing the condyles from the femur and tibia and flushing the bones with DMEM containing 5% FBS (Hyclone). The bone marrow cells were then collected and plated in IMDM with 15% FBS, as well as IL-4, IL-7, SCF (all 10 μg/ml; Peprotech), and

doxycycline (2 μg/ml). Four days later, the medium was changed to neural induction medium for iNSC formation. For splenocytes, the spleen was manually dissociated in RPMI containing 15% FBS and filtered through a 100 μM filter. Cells were collected by centrifugation and plated in neural induction medium for iNSC formation. For the isolation of liver cells, the mice were first perfused with 50 ml HBSS and then with 50 ml HBSS containing collagenase type IV (100 U/ml; Sigma). The liver was dissociated in DMEM with BSA (2 g/L) and filtered two times through a 100 μM filter. Cells were collected by centrifugation at 30g for 3 minutes at 4°C, washed twice, and plated in neural induction medium.

Lentiviral cloning and infections

To create lentiviral vectors, genes of interest were amplified by PCR either from cDNA libraries or from cDNA expression vectors using primers flanked by EcoRI restriction sites (MfeI was used instead of EcoRI for genes that contained internal EcoRI restriction sites). The PCR products were cloned into the TOPO-TA cloning vector (Life Technologies) following the manufacturer's instructions. The genes were then excised from the TOPO-TA vector and ligated into the EcoRI site of the FUW-TetO lentiviral backbone in which transgene expression is controlled by the tetracycline-reponsive operator sequence and a minimal CMV promoter (TetO) (Beard et al., 2006).

Lentivirus was generated in 6-well plates by co-transfecting 293T cells with 2.5 μg of lentiviral vector, 0.625 μg of pMD2.G, and 1.875 μg psPAX2 (packaging vectors from Addgene) using Fugene 6 (Promega) according to the manufacturer's instructions.

MEF medium was replaced 16-24 hours after transfection. Viral supernatants were harvested 48 and 72 hours after transfection and filtered through a 0.45 μm filter. MEFs were transduced by adding a 1:1 mixture of viral supernatants and MEF medium to the cells in the presence of 8 μg/ml polybrene (Sigma). After 24 hours, the MEF medium was replaced and on the following day doxycycline (Sigma) was added (2 ug/ml).

Neural cell culture and differentiation

Primary-derived neural stem cells and established iNSCs were cultured in N2 medium (Okabe et al., 1996) [DMEM/F-12 medium containing insulin (5 μg/ml) (Sigma), transferrin (100 μg/ml) (Sigma), sodium selenite (30 nM) (Sigma), progesterone (20 nM) (Sigma), putrescine (100 nM) (Sigma), and penicillin and streptomycin (100 μg/ml) (Life Technologies)] supplemented with 20 ng/ml epidermal growth factor (EGF) (R & D systems), 20 ng/ml basic fibroblast growth factor (bFGF) (Sigma), and 1 μg/ml laminin (Life Technologies). NSC medium was replenished every 24-48 hours, and cells were passaged every 2-3 days.

For neuronal differentiation, cells were plated on polyornithine- and laminin-coated plates and EGF withdrawn for 2 days followed by bFGF withdrawl and the addition of BDNF (10 μg/ml; Peprotech), ascorbic acid (200 nM; Sigma), and NT3 (10 μg/ml; Peprotech) for an additional 10-14 days (Their et al., 2012). For electrophysiology experiments, the differentiation medium was supplemented with astrocyte conditioned medium (1:4) for 2 more weeks before analysis. Astrocyte differentiation was performed by withdrawing growth factors and supplementing the

medium with 5% FBS for 7-10 days (Conti et al., 2005). For oligodendrocyte differentiation 200,000 cells were plated on polyornithine- and laminin-coated 12-well plates and cultured with bFGF (10 μg/ml), PDGF (10 μg/ml; Peprotech), and forskolin (10 nM; Sigma) for 5 days and then with ascorbic acid (200 nM) and T3 (30 ng/ml; Sigma) for 4 days (Lujan et al., 2012; Glaser et al., 2007).

Control NSC derivation

The forebrain cortex of E12.5 embryos was collected in Hank's buffered saline solution (HBSS). Tissue was dissociated by tritruation and then incubated in HBSS for 10 minutes at room temperature. Cells were collected by centrifugation and plated in N2 containing EGF (20 ng/ml), bFGF (20 ng/ml), and laminin (1 μg/ml) and then cultured for stable cell lines.

iNSC reprogramming

For the generation of iNSCs, transduced MEFs were grown for 4 days in MEF medium supplemented with 2 μg/ml doxycycline (Sigma) before being switched to neural induction medium [N2 medium plus 10 ng/ml EGF, 10 ng/ml FGF (Sigma), 1 μg/ml laminin, and 2 μg/ml doxycycline]. The cells were grown in neural induction medium for 2-3 weeks before the addition of ITSFn selection medium [DMEM/F-12 medium containing insulin (25 μg/ml), transferrin (50 μg/ml), sodium selenite (30 nM), fibronectin (5 μg/ml) (Sigma), and penicillin and streptomycin (100 μg/ml)] (Okabe et al., 1996). The selection medium was supplemented with doxycycline (2 μg/ml) for the first

4 days, and on day 10 the cultures were dissociated by incubating them with 0.25% trypsin (Sigma) for 5-10 minutes. The trypsin was quenched with 10% serum (Hyclone), and the cells were collected by centrifugation and washed once with DMEM/F-12. The cells were then replated to plates coated with polyornithine (15 μg/ml) and laminin (1 μg/ml) (for 24 hours each) and then grown in neural expansion medium [N2 supplemented with 20 ng/ml EGF, 20 ng/ml bFGF, and 1 μg/ml laminin]. Medium was replenished every other day for 2-3 weeks until NSC-like foci became visible, after which cells were fed daily to promote iNSC growth. *Sox2*-GFP+ cells were sorted directly into polyornithine- and laminin-coated plates using the BD FACSAria IIU cell sorter (BD Biosciences). The cells were split at confluence for P1.

Electrophysiology

Artificial cerebro-spinal fluid (ACSF) [125 mM NaCl, 3 mM KCl, 1.25 mM NaH_2PO_4, 25 mM $NaHCO_3$, 1 mM $MgCl_2$, 2.5 mM $CaCl_2$, and 20 mM Dextrose, with osmolality adjust to 312 ± 3mOsm] was continuously bubbled with 95% O_2 and 5% CO_2 and perfused over individual coverslips during the recordings. Putative neurons within a mixed culture were visually identified for whole-cell patch clamp using differential interference contrast (DIC) optics on an Olympus BX61 microscope (Olympus Corp., USA). Patch pipettes, pulled from borosilicate capillaries (Sutter Instruments, Novato, CA, USA), were filled with a solution containing 120 mM K-Gluconate, 10 mM KCl, 10 mM HEPES, 4 mM Mg-ATP, 0.3 mM Na-GTP, 10 mM Na_2-Creatinine Phosphate, with pH 7.3 and osmolality adjusted to 300 ± 3 mOsm with Sucrose. Data was acquired

using a Multiclamp 700B (Molecular Devices, Sunnyvale, CA, USA) amplifier, low pass filtered at 10 kHz (current clamp) or 2 kHz (voltage clamp), and digitized at 10 kHz with a Digidata 1440 system (Molecular Devices). During current clamp recordings, a constant hyperpolarizing current injection was applied to hold the membrane potential at approximately -65mV, and 500ms long depolarizing current steps of varying amplitude were delivered to evoke action potentials. To detect voltage-gated ion currents, cells were continuously held at -70mV in voltage clamp mode while briefly delivering voltage pulses from -100mV to 50mV, in 10mV increments. Leak current and capacitive transients during voltage steps were subtracted from raw traces. All data were acquired and analyzed using pClamp10 software (Molecular Devices).

Immunostaining

For NSC and iNSC immunostaining, cells were washed twice with HBS, fixed in 4% paraformaldehyde for 20 minutes at room temperature, and then washed twice in PBS containing magnesium and calcium ions (PBS+). Cells were blocked by incubating them in PBS+ containing 5% normal donkey serum (Jackson Immunoresearch) and 0.3% Triton X-100 (Sigma) for 60 minutes at room temperature. Antibodies were diluted in a solution of PBS+ with 1% BSA (Sigma) and 0.3% Triton X-100. Primary antibodies were incubated overnight at 4°C, and secondary antibodies were incubated for 60 minutes at room temperature in the dark. Cells were washed 3 times with PBS+ after the primary antibody incubation and twice after secondary antibody incubation. To stain nuclei, cells were incubated with 4',6-diamidino-2-phenylindole (DAPI) for 5-10 minutes

and subsequently washed with PBS+. The following primary antibodies were used: rabbit anti-GFAP (DAKO, 1:2000), chicken anti-GFP (Aves Labs, 1:1000), mouse anti-MAP2 (Sigma, 1:1000), rat anti-MBP (Abcam, 1:500), mouse anti-NESTIN (Developmental Studies Hybridoma Bank, 1:500), mouse anti-O1 (R&D systems, 1:100), mouse anti-O4 (R&D systems, 1:100), rabbit anti-PAX6 (Covance, 1:250), mouse anti-TUJ1 (Covance, 1:1000).

iPS reprogramming

The Moloney viral vectors pMXs-*Oct4*, *Klf4*, *Myc*, *Nanog*, and *Sall4* were purchased from Addgene (Takahashi and Yamanaka, 2006). pMXs-*Esrrb* was generated by digesting TetO-*Esrrb* (Buganim et al., 2012b) with EcoRI and then ligating it into the EcoRI site of pMXs. For transductions, equal amounts of pCLeco and either *Oct4*, *Klf4*, *Myc*, *Nanog*, *Sall4*, or *Esrrb* retroviral vectors were co-transfected into 293T cells using the Fugene 6 transfection reagent (Promega). One day after transfection, the 293T culture medium was exchanged for N2 medium supplemented with 20 ng/ml EGF, 20 ng/ml bFGF, 1 μg/ml laminin, and 5 μg/ml fibronectin. Viral supernatants were collected 48 and 72 hours after transfection and pooled for infection.

The infected cells were grown in NSC medium for 4 days and then grown in ES medium [DMEM supplemented with 10% FBS (Hyclone), penicillin and streptomycin (100 μg/ml) (Life Technologies), L-glutamine (2mM) (Life Technologies), nonessential amino acids (Life Technologies), 0.1 mM β-mercaptoethanol, and leukemia inhibitory factor (Lif)]. When pre-iPS colonies began to emerge, the culture was switched to

serum-free 2i/Lif medium [1:1 mixture of DMEM/F-12 (Life Technologies) and Neurobasal (Life Technologies) base mediums plus N2 supplement (Life Technologies), B27 supplement (Life Technologies), recombinant human LIF, 2 mM L-glutamine (Life Technologies), 1% nonessential amino acids (Life Technologies), 0.1 mM β-mercaptoethanol (Sigma), penicillin and streptomycin (100 μg/ml) (Life Technologies), 5 μg/mL BSA (Sigma), 1 μM PD0325901 (Stemgent), and 3 μM CHIR99021 (Stemgent)] (Hanna et al., 2010). iPS colonies were manually picked and after 1 passage in 2i/lif medium, they were cultured in ES medium.

Teratomas and blastocyst injections

For teratoma analysis, cells were dissociated in 0.25% trypsin and then collected in ES medium. 5×10^5 cells were injected subcutaneously into both flanks of recipient immunocomprimised SCID mice (Brambrink et al., 2008). Tumors approximately 1 cm in diameter were harvested 3-4 weeks after injection for paraffin sectioning and stained with hematoxylin and eosin. Blastocyst injections were performed as described (Wernig et al., 2008b) except that E14.5 embryos were extracted from pregnant females for the isolation of MEFs.

VDJ rearrangement analysis

IgH, *Igκ*, and *Igλ* rearrangements were PCR amplified as previously described (Hanna et al., 2008; Chang et al., 1992; Cobaleda et al., 2007). To characterize individual VDJ rearrangements, PCR fragments were cloned into the TOPO vector, and

at least 8 clones of an individual PCR band were sequenced. Sequences were analyzed using the IMGT database (www.imgt.org) (Brochet et al., 2008). For D_H-J_H rearrangements, the sequencing result was appended to a known V_H segment for IMGT analysis.

Chromatin Immunoprecipitation (ChIP)

ChIPs were performed as previously described (Lee et al., 2006). Briefly, MEF, NSC, and iNSC-13F cells were grown to a final count of 20 million cells and crosslinked for 12 minutes at room temperature by the addition of one-tenth volume of 11% formaldehyde solution (11% formaldehyde, 50mM HEPES pH 7.3, 100 mM NaCl, 1 mM EDTA pH 8.0, 0.5 mM EGTA pH8.0). Cells were washed twice with PBS, scraped, and frozen in liquid nitrogen. 20 µl of Dynal magnetic beads (Sigma) were blocked with 0.5% BSA (w/v) in PBS and then bound with 5 µg of H3K27ac antibody (Abcam, ab4729) overnight at 4°C with rotation. Nuclear extracts were prepared by resuspending crosslinked cells with 50 mM HEPES pH 7.3, 140 mM NaCl, 1 mM EDTA, 10% glycerol, 0.5% NP-40, and 0.25% Triton X-100 and rotating them for 10 minutes at 4°C, followed by centrifugation at 1350g for 5 min. Nuclei were resuspended in sonication buffer (50 mM Tris-HCl pH 7.5, 140 mM NaCl, 1 mM EDTA, 1% Triton X-100, 0.1% Na-deoxycholate, 0.1% SDS) and sonicated using Bioruptor® Standard (Diagenode) for 20 x 30 second pulses (30 second pause between pulses). Sonicated lysates were cleared and incubated overnight at 4°C with magnetic beads bound with antibody to enrich for DNA fragments bound by the H3K27ac mark. Beads were washed two times with sonication buffer, one time with sonication buffer with 500 mM NaCl, one time with

LiCl wash buffer (20 mM Tris pH 8.0, 1 mM EDTA, 250 mM LiCl, 0.5% NP-40, 0.5% Na-deoxycholate), and one time with TE. DNA was eluted in elution buffer. Crosslinks were reversed overnight at 65°C. RNA and protein were digested using RNase A and Proteinase K, respectively, and DNA was purified with phenol:chloroform extraction and ethanol precipitation.

Identifying ChIP-Seq enriched regions

All ChIP-seq datasets were aligned using Bowtie (version 0.12.2, Langmead et al., 2009) to the build version NCBI37/MM9 of the mouse genome with -k 1 -m 1 -n 2 setting. The MACS version 1.4.1 (Model-based analysis of ChIP-Seq) (Zhang et al., 2008) peak finding algorithm was used to identify regions of ChIP-Seq enrichment over background. A p-value threshold of enrichment of 1×10^{-9} was used for all data sets.

Defining active enhancers

Active enhancers were defined as regions of enrichment for H3K27ac outside of promoters (greater than 5 kb away from any transcriptional start site (TSS)). H3K27ac is a histone modification associated with active enhancers (Creyghton et al., 2010; Rada-Iglesias et al., 2011).

ChIP-Seq density heatmaps and composite ChIP-Seq density profiles

In order to display ChIP-Seq levels at enhancers, a heatmap representation was used. The enhancer regions of NSCs and MEFs were aligned at the center in the

composite view of signal density profile. The average ChIP-Seq read density (rpm/bp) around +/- 5 kb centered on the centers in 50 bp bin was calculated and displayed.

Microarray analysis

All expression profiles including the previous published expression datasets were processed together to generate Affymetrix MAS5-normalized probe set values. We processed all CEL files by using the probe definition ("mouse4302 cdf") and the standard MAS5 normalization technique within the affy package in R to get probe set expression values.

The expression profiles were compared and clustered by hierarchical clustering using average linkage. The distance matrix was calculated using Pearson correlation coefficients of the top 50 percent of probe sets with the largest coefficients of variation across expression profiles.

The differentially expressed probe sets between the published datasets of mouse embryonic fibroblasts (MEFs) and mouse neural precursor cells (NPCs) were determined using a linear model within the limma package in R. The empirical Bayes approach was used to estimate variances. The differentially expressed probe sets were required to have absolute value of log2-fold change greater than 2 and FDR-adjusted p-value less than 0.01.

Previously published gene expression datasets

Two previously published datasets using the Affymetrix Mouse Genome 430 2.0

Array (platform ID GPL1261) microarray platform were obtained from the Gene Expression Omnibus (http://www.ncbi.nlm.nih.gov/geo/) database (see below). For Mikkelsen et al. (2007), data were obtained from the GEO database accession GSE8024. For Cahoy et al. (2008), data were obtained from the GEO database accession GSE15148.

Previously Published Datasets

Cell Type	GEO ID	Name	Reference
Neural precursor cells	GSM198065	ES derived NPC Replicate 1	Mikkelsen et al., 2007
Neural precursor cells	GSM198066	ES derived NPC Replicate 2	Mikkelsen et al., 2007
Neural precursor cells	GSM198067	ES derived NPC Replicate 3	Mikkelsen et al., 2007
Mouse Embryonic Stem Cells	GSM198062	Mouse Embryonic Stem Cells Replicate 1	Mikkelsen et al., 2007
Mouse Embryonic Stem Cells	GSM198063	Mouse Embryonic Stem Cells Replicate 2	Mikkelsen et al., 2007
Mouse Embryonic Stem Cells	GSM198064	Mouse Embryonic Stem Cells Replicate 3	Mikkelsen et al., 2007
Mouse embryonic fibroblasts	GSM198070	Mouse embryonic fibroblasts Replicate 1	Mikkelsen et al., 2007
Mouse embryonic fibroblasts	GSM198072	Mouse embryonic fibroblasts Replicate 2	Mikkelsen et al., 2007
Oligodendrocytes	GSM241889	Oligodendrocytes	Cahoy et al., 2008
Oligodendrocytes	GSM241891	Oligodendrocytes	Cahoy et al., 2008
Oligodendrocytes	GSM241892	Oligodendrocytes	Cahoy et al., 2008
Oligodendrocytes	GSM241917	Oligodendrocytes	Cahoy et al., 2008
Astrocytes	GSM241912	Astrocytes	Cahoy et al., 2008
Astrocytes	GSM241914	Astrocytes	Cahoy et al., 2008
Astrocytes	GSM241926	Astrocytes	Cahoy et al., 2008
Neurons	GSM241904	Neurons	Cahoy et al., 2008
Neurons	GSM241896	Neurons	Cahoy et al., 2008

Defined factors screened for iNSC formation in MEFs

Gene Name	Species	Genbank Accession
Ascl1	Mouse	NM_008553
Bmi1	Mouse	NM_007552
Brn2	Mouse	NM_008899
DN-REST (P73 REST)*	Human	NM_005612 (REST)
Hes1	Mouse	NM_008235
Hes3	Mouse	NM_008237
Hes5	Mouse	NM_010419
Klf4	Mouse	NM_010637
Lhx2	Mouse	NM_010710
MEF2CA**	Human	NM_002397 (MEF2C)
mir124a	Human	NR_029668
c-Myc	Mouse	NM_010849
Myt1l	Mouse	NM_001093775
Ngn2	Mouse	NM_009718
NOTCH- intracellular domain (ICD)	Human	NM_017617 (NOTCH1)
Olig1	Mouse	NM_016968
Olig2	Mouse	NM_016967
Pax6	Mouse	NM_001244198
PLAGL1	Human	NM_002656
PLZF	Human	NM_006006
Rfx4	Mouse	NM_001024918
Sox1	Mouse	NM_009233
Sox2	Mouse	NM_011443
SOX3	Human	NM_005634
Sox9	Mouse	NM_011448
Zic1	Mouse	NM_009573

* Dominant-Negative REST. Chong el al. 1995

** Constitutively active MEF2. Li et al. 2008

Primers for PCR genotyping the transduced factors

Gene Name	Forward Primer	Reverse Primer
Ascl1	ATCCACGCTGTTTTGACCTC	GTTTGCAGCGCATCAGTTC
Bmi1	GTGTACGGTGGGAGGCCTAT	TGCAACTTCTCCTCGGTCTT
Brn2	GTGTACGGTGGGAGGCCTAT	CACCCTGCTGTACCACCAC
DN-REST	GAATCTGGCTCTTCCACTGC	GAGGTTTAGGCCCATTGTGA
Foxg1	GTGTACGGTGGGAGGCCTAT	CGCCCCTTTCTTCTCCTC
Hes1	ATCCACGCTGTTTTGACCTC	GTCACCTCGTTCATGCACTC
Hes3	GTGTACGGTGGGAGGCCTAT	AGGCAAGGGTTGAGAACAGA
Hes5	GTGTACGGTGGGAGGCCTAT	CAGGAGTAGCCCTCGCTGTA
Klf4	GTGTACGGTGGGAGGCCTAT	CTAGGTCCAGGAGGTCGTTG
Lhx2	GCGAATACCCAGCACACTTT	TAAAAGGTTGCGCCTGAACT
MEF2CA	CTTATGAGCTGAGCGTGCTG	GTGAGCCAGTGGCAATAGGT
mir124a	ATCCACGCTGTTTTGACCTC	AATCAAGGTCCGCTGTGAAC
c-Myc	GTGTACGGTGGGAGGCCTAT	ACCGCAACATAGGATGGAGA
Myt1l	GTGTACGGTGGGAGGCCTAT	CCCCTTGCTCATCATTGTCT
Ngn2	ATCCACGCTGTTTTGACCTC	GTCTTCTTGATGCGCTGCAC
NOTCH ICD	CATGGACGACAACCAGAATG	CATGTTGTCCTGGATGTTGG
Olig1	ATCCACGCTGTTTTGACCTC	GTGGCAATCTTGGAGAGCTT
Olig2	ATCCACGCTGTTTTGACCTC	GGGCTCAGTCATCTGCTTCT
PLAGL1	CAAGTGTGTGCAGCCTGACT	ATCTCTGGGCACAGAACTGG
PLZF	GTGTACGGTGGGAGGCCTAT	CTGGATGGTCTCCAGCATCT
Rfx4	GTTACTGGAGGAACCCGACA	GAATATGCCACCGTCTGCTT
Sox1	GTGTACGGTGGGAGGCCTAT	GTCCTTCTTGAGCAGCGTCT
Sox2	GTGTACGGTGGGAGGCCTAT	CTCCGGGAAGCGTGTACTTA
SOX3	GTGTACGGTGGGAGGCCTAT	CTGCGTTCGCACTACTCTTG
Sox9	AGGAAGCTGGCAGACCAGTA	CCCTCTCGCTTCAGATCAAC
Zic1	TCTGCTTCTGGGAGGAGTGT	CTGTTGTGGGAGACACGATG

Primers used for qPCR analysis

Gene	Forward Primer	Reverse Primer
AAT	GGCTGACCTCTCCGGAAT	GTCAGCACGGCCTTATGC
Actin	CTTCTTTGCAGCTCCTTCGTT	TTCTGACCCATTCCCACCA
Albumin	AGTGTTGTGCAGAGGCTGAC	TTCTCCTTCACACCATCAAGC
Brn2	AGCAGTTCGCCAAGCAATTC	CGAGAACACGTTGCCGTACA
Col5a2	TAGAGGAAGAAAGGGACAAAAAGG	GTTACAACAGGCACTAATCCTGGTT
Gapdh	TTCACCACCATGGAGAAGGC	CCCTTTTGGCTCCACCCT
Ncan	GGACAGACAACACAGGACTGC	CCCACCTGCGAAGAAATTAT
Nestin	GATCGCTCAGATCCTGGAAG	CCAAGAGAAGCCTGGGAACT
Olig2	AGACCGAGCCAACACCAG	AAGCTCTCGAATGATCCTTCTTT
Pax5	CGCGTGTTTGAGAGACAGCACTACT	GTCTCGGCCTGTGACAATAGGGTAG
Pax6	GAAGGAGGGGGAGAGAACAC	CTCCAGAGCCTCAATCTGCT
Pu.1	CGGATGACTTGGTTACTTACG	GTAGGAAACCTGGTGACTGAG
Sox1	TGTAATCCGGGTGTTCCTTC	AACCCCAAGATGCACAACTC
Sox2	ACTTTTGTCCGAGACCGAGA	CTCCGGGAAGCGTGTACTTA
Sox3	GCCTTGTACCGAAGATGAGG	ACAAAACCCCGACAGTTACG
Thy1	CGAATCCCATGAGCTCCAAT	CCAGCTTGTCTCTATACACACTGATA

SUPPLEMENTAL REFERENCES

Beard, C., Hochedlinger, K., Plath, K., Wutz, A., and Jaenisch, R. (2006). Efficient method to generate single-copy transgenic mice by site-specific integration in embryonic stem cells. Genesis 44, 23–28.

Brochet, X., Lefranc, M.-P., and Giudicelli, V. (2008). IMGT/V-QUEST: the highly customized and integrated system for IG and TR standardized V-J and V-D-J sequence analysis. Nucleic Acids Res. 36, W503–W508.

Buganim, Y., Faddah, D.A., Cheng, A.W., Itskovich, E., Markoulaki, S., Ganz, K., Klemm, S.L., van Oudenaarden, A., and Jaenisch, R. (2012b). Single-cell expression analyses during cellular reprogramming reveal an early stochastic and a late hierarchic phase. Cell 150, 1209–1222.

Chang, Y., Paige, C.J., and Wu, G.E. (1992). Enumeration and characterization of DJH structures in mouse fetal liver. Embo J. *11*, 1891–1899.

Carey, B.W., Markoulaki, S., Beard, C., Hanna, J., and Jaenisch, R. (2010). Single-gene transgenic mouse strains for reprogramming adult somatic cells. Nat. Methods 7, 56–59.

Carey, B.W., Markoulaki, S., Hanna, J.H., Faddah, D.A., Buganim, Y., Kim, J., Ganz, K., Steine, E.J., Cassady, J.P., Creyghton, M.P., et al. (2011). Reprogramming factor stoichiometry influences the epigenetic state and biological properties of induced pluripotent stem cells. Cell Stem Cell 9, 588–598.

Chong, J.A., Tapia-Ramírez, J., Kim, S., Toledo-Aral, J.J., Zheng, Y., Boutros, M.C., Altshuller, Y.M., Frohman, M.A., Kraner, S.D., and Mandel, G. (1995). REST: a mammalian silencer protein that restricts sodium channel gene expression to neurons. Cell 80, 949–957.

Cobaleda, C., Jochum, W., and Busslinger, M. (2007). Conversion of mature B cells into T cells by dedifferentiation to uncommitted progenitors. Nature *449*, 473–477.

Conti, L., Pollard, S.M., Gorba, T., Reitano, E., Toselli, M., Biella, G., Sun, Y., Sanzone, S., et al. (2005). Niche-Independent Symmetrical Self-Renewal of a Mammalian Tissue Stem Cell. Plos Biol 3, e283.

Langmead, B., Trapnell, C., Pop, M., and Salzberg, S.L. (2009). Ultrafast and memory-efficient alignment of short DNA sequences to the human genome. Genome Biol. 10, R25.

Lee, T.I., Jenner, R.G., Boyer, L.A., Guenther, M.G., Levine, S.S., Kumar, R.M., Chevalier, B., Johnstone, S.E., Cole, M.F., Isono, K.-I., et al. (2006). Control of developmental regulators by Polycomb in human embryonic stem cells. Cell 125, 301–313.

Li, Z., McKercher, S.R., Cui, J., Nie, Z., Soussou, W., Roberts, A.J., Sallmen, T., Lipton, J.H., Talantova, M., Okamoto, S.I., et al. (2008). Myocyte Enhancer Factor 2C as a Neurogenic and Antiapoptotic Transcription Factor in Murine Embryonic Stem Cells. J. Neurosci. 28, 6557–6568.

Rada-Iglesias, A., Bajpai, R., Swigut, T., Brugmann, S.A., Flynn, R.A., and Wysocka, J. (2011). A unique chromatin signature uncovers early developmental enhancers in humans. Nature 470, 279–283.

Zhang, Y., Liu, T., Meyer, C.A., Eeckhoute, J., Johnson, D.S., Bernstein, B.E., Nusbaum, C., Myers, R.M., Brown, M., Li, W., et al. (2008). Model-based analysis of ChIP-Seq (MACS). Genome Biol. 9, R137.